

# Casimir effect for fermion condensate in conical rings

A. A. Saharian<sup>1</sup>, T. A. Petrosyan<sup>1</sup>, A. A. Hovhannisyan<sup>2</sup>

<sup>1</sup>*Department of Physics, Yerevan State University,  
1 Alex Manoogian Street, 0025 Yerevan, Armenia*

<sup>2</sup>*Institute of Applied Problems of Physics NAS RA,  
25 Nersessian Street, 0014 Yerevan, Armenia*

## Abstract

The fermion condensate (FC) is investigated for a (2+1)-dimensional massive fermionic field confined on a truncated cone with an arbitrary planar angle deficit and threaded by a magnetic flux. Different combinations of the boundary conditions are imposed on the edges of the cone. They include the bag boundary condition as a special case. By using the generalized Abel-Plana-type summation formula for the series over the eigenvalues of the radial quantum number, the edge-induced contributions in the FC are explicitly extracted. The FC is an even periodic function of the magnetic flux with the period equal to the flux quantum. Depending on the boundary conditions, the condensate can be either positive or negative. For a massless field the FC in the boundary-free conical geometry vanishes and the nonzero contributions are purely edge-induced effects. This provides a mechanism for time-reversal symmetry breaking in the absence of magnetic fields. Combining the results for the fields corresponding to two inequivalent irreducible representations of the Clifford algebra, the FC is investigated in the parity and time-reversal symmetric fermionic models and applications are discussed for graphitic cones.

**Keywords:** fermion condensate; Casimir effect; conical geometry; graphene

## 1 Introduction

Field theoretical fermionic models in (2+1)-dimensional spacetime appear as long-wavelength effective theories describing a relatively large class of condensed matter systems, including graphene family materials, topological insulators, Weyl semimetals, high-temperature superconductors, ultracold atoms confined by lattice potentials, and nano-patterned 2D electron gases [1, 2]. In the low-energy approximation, the corresponding dynamics of charge carriers is governed with fairly good accuracy by the Dirac equation, where the velocity of light is replaced by the Fermi velocity [3]-[5]. The latter is much less than the velocity of light, and this presents a unique possibility for studying relativistic effects.

Among the most interesting topics in quantum field theory is the dependence of the properties of the vacuum state on the geometry of the background spacetime. The emergence of Dirac fermions in the abovementioned condensed matter systems and availability of a number of mechanisms to control the corresponding effective geometry provide an important opportunity to observe different kinds of field-theoretical effects induced by the spatial geometry and topology. In particular, it is of special interest to investigate the influence of boundaries on the physical characteristics of the ground state. This influence can be described by imposing appropriate boundary conditions on the field operator. Those conditions modify the spectrum of vacuum fluctuations and, as a consequence, the vacuum expectation values of physical observables are shifted by an amount that depends on the bulk and

boundary geometries and on the boundary conditions. The general class of those effects is known under the name of the Casimir effect (for reviews see [6]-[10]). In recent years, the Casimir effect for the electromagnetic field in physical systems with graphene structures as boundaries has been widely discussed in the literature (see references [11]-[34] and references [35]-[37] for reviews). By using external fields, different electronic phases can be realized in Dirac materials. The magnitude and the scaling law of the corresponding Casimir forces are essentially different for those phases [38]. New interesting features arise in interacting fermionic systems [39]-[44].

Graphene family materials also offer a unique opportunity to investigate the boundary-induced and topological Casimir effects for a fermionic field. On the edges of graphene nanoribbons boundary conditions are imposed on the effective fermionic field that ensure the zero flux of the quasiparticles. Those conditions are sources for the Casimir-type contributions to the expectation values of physical characteristics of the ground state. Similarly, the periodicity conditions along compact dimensions imposed on the fermionic field in graphene nanotubes and nanorings give rise to the topological Casimir effect for those characteristics. As such characteristics, in [45, 46, 47] the fermion condensate, the expectation values of the current density and of the energy-momentum tensor have been studied. The edge-induced Casimir contributions in finite length carbon nanotubes were discussed in [48]-[50]. Tubes with more complicated curved geometries have been considered in [51]-[54]. These geometries provide exactly solvable examples to model the combined influence of gravity and topology on the properties of quantum matter. Note that various mechanisms have been considered in the literature that allow to control the effective geometry in graphene type materials [55]-[58].

As background geometry, in the present paper we consider a 2-dimensional conical space with two circular boundaries (conical ring). The corresponding spacetime is flat and is a (2+1)-dimensional analog of the cosmic string geometry. We investigate the influence of the edges and of the magnetic flux, threading the ring, on the fermion condensate (FC). The corresponding vacuum expectation values of the fermionic charge and current densities have been recently studied in [59]. Among the interesting applications of the setup under consideration are the graphitic cones. They are obtained from a graphene sheet by cutting a sector with the angle  $\pi n_c/3$ ,  $n_c = 1, 2, \dots, 5$ , and then appropriately gluing the edges of the remaining sector. The opening angle of the cone, obtained in this way, is given by  $\phi_0 = 2\pi(1 - n_c/6)$ . The graphitic cones with the angle  $\phi_0$  for all the values corresponding to  $n_c = 1, 2, \dots, 5$ , have been observed experimentally [60]-[62]. The corresponding electronic properties were studied in references [63]-[70]. Our main interest here is the investigation of the Casimir-type contributions to the FC induced by the edges of a conical ring for general values of the opening angle. The ground state fermionic expectation values for limiting cases of the geometry under consideration, corresponding to boundary-free cones and to cones with a single circular edge, have been examined in references [71]-[76]. In particular, the FC has been discussed in [74]. The effects of finite temperature on the FC were investigated in [77, 78]. The formation of the FC in models with a background scalar field has been recently discussed in [79, 80]. The vacuum expectation values for the charge and current densities on planar rings have been studied in [81].

The paper is organized as follows. In the next section we describe the geometry and present the complete set of fermionic modes. Based on those modes, the FC is evaluated in Section 3. Various representations are provided for the edge-induced contributions and numerical results are presented. In Section 4, by combining the results for the fields realizing two inequivalent irreducible representations of the Clifford algebra, we consider the FC in parity and time-reversal symmetric models. Applications to graphitic cones are discussed. The main results are summarized in Section 5.

## 2 Geometry and the field modes

We consider a charged fermionic field in (2+1)-dimensional conical spacetime described by the coordinates  $x^0 = t$ ,  $x^1 = r$ ,  $x^2 = \phi$ , with  $r \geq 0$ ,  $0 \leq \phi \leq \phi_0$ . The corresponding metric tensor is given

by

$$g_{\mu\nu} = \text{diag}(1, -1, -r^2). \quad (1)$$

For  $\phi_0 = 2\pi$  this metric tensor corresponds to (2+1)-dimensional Minkowski spacetime. For  $\phi_0 < 2\pi$  one has a planar angle deficit  $2\pi - \phi_0$  and the spacetime is flat everywhere except at the apex  $r = 0$  where it has a delta type curvature singularity. In (2+1)-dimensional spacetime there are two inequivalent irreducible representations of the Clifford algebra with the  $2 \times 2$  Dirac matrices  $\gamma_{(s)}^\mu = (\gamma^0, \gamma^1, \gamma_{(s)}^2)$ , where  $s = \pm 1$  correspond to two representations. We will use the representations with  $\gamma^0 = \text{diag}(1, -1)$  and

$$\gamma^1 = i \begin{pmatrix} 0 & e^{-iq\phi} \\ e^{iq\phi} & 0 \end{pmatrix}, \quad \gamma_{(s)}^2 = \frac{s}{r} \begin{pmatrix} 0 & e^{-iq\phi} \\ -e^{iq\phi} & 0 \end{pmatrix}, \quad (2)$$

where  $q = 2\pi/\phi_0$ . Note that one has the relation  $\gamma_{(s)}^2 = -is\gamma^0\gamma^1/r$ .

Let  $\psi_{(s)}$ ,  $s = \pm 1$ , be two-component spinor fields corresponding to two inequivalent irreducible representations of the Clifford algebra. In the presence of an external gauge field  $A_\mu$ , the corresponding Lagrangian density has the form

$$L_{(s)} = \bar{\psi}_{(s)}(i\gamma_{(s)}^\mu D_{(s)\mu} - m_{(s)})\psi_{(s)} \quad (3)$$

with the covariant derivative operator  $D_{(s)\mu} = \partial_\mu + \Gamma_{(s)\mu} + ieA_\mu$ , the spin connection  $\Gamma_{(s)\mu}$  and the Dirac adjoint  $\bar{\psi}_{(s)} = \psi_{(s)}^\dagger \gamma^0$ . We are interested in the effects of two circular boundaries  $r = a$  and  $r = b$ ,  $a < b$ , on the fermion condensate (FC)

$$\langle 0 | \bar{\psi}_{(s)} \psi_{(s)} | 0 \rangle \equiv \langle \bar{\psi}_{(s)} \psi_{(s)} \rangle, \quad (4)$$

where  $|0\rangle$  corresponds to the vacuum state. On the edges the boundary conditions

$$\left(1 + i\lambda_r^{(s)} n_\mu^{(r)} \gamma_{(s)}^\mu\right) \psi_{(s)} = 0, \quad r = a, b, \quad (5)$$

will be imposed with  $\lambda_r^{(s)} = \pm 1$  and with  $n_\mu^{(r)}$  being the inward pointing unit vector normal to the corresponding boundary. We can pass to the new set of fields  $\psi'_{(s)}$  defined as  $\psi'_{(+1)} = \psi_{(+1)}$ ,  $\psi'_{(-1)} = \gamma^0 \gamma^1 \psi_{(-1)}$ . The corresponding Lagrangian density is presented as  $L_{(s)} = \bar{\psi}'_{(s)}(i\gamma^\mu D_\mu - sm_{(s)})\psi'_{(s)}$ , where  $\gamma^\mu = \gamma_{(+1)}^\mu$  and  $D_\mu = D_{(+1)\mu}$ . The boundary conditions are transformed to  $\left(1 + i\lambda_r^{(s)'} n_\mu^{(r)} \gamma^\mu\right) \psi'_{(s)} = 0$ , with  $\lambda_r^{(s)'} = s\lambda_r^{(s)}$  and  $r = a, b$ . By taking into account that  $\psi_{(-1)} = \gamma^0 \gamma^1 \psi'_{(-1)}$ , for the FC we get  $\langle \bar{\psi}_{(s)} \psi_{(s)} \rangle = \langle \bar{\psi}'_{(s)} \psi'_{(s)} \rangle$ . The boundary condition (5) with  $\lambda_r^{(s)} = 1$  has been used in MIT bag models to confine the quarks inside hadrons (for a review see [82]). In condensed matter applications it is known as infinite mass or hard wall boundary condition [83]. As it has been mentioned in [83], another possibility to confine the fermions corresponds to the condition (5) with  $\lambda_r^{(s)} = -1$ . Note that one has  $\left(in_\mu^{(r)} \gamma_{(s)}^\mu\right)^2 = 1$  and for the eigenvalues of the matrix  $in_\mu^{(r)} \gamma_{(s)}^\mu$  we get  $\pm 1$ . Here, the upper and lower signs correspond to the boundary conditions (5) with  $\lambda_r^{(s)} = -1$  and  $\lambda_r^{(s)} = 1$ , respectively. More general boundary conditions for the confinement of fermions, containing additional parameters, have been discussed in [84]-[89].

In the discussion below, the investigation for the FC will be presented in terms of the fields  $\psi'_{(s)} = \psi$ , omitting the prime and the index. So, we consider a two-component fermionic field  $\psi(x)$  obeying the Dirac equation

$$(i\gamma^\mu D_\mu - sm)\psi(x) = 0, \quad (6)$$

and the boundary conditions

$$\left(1 + i\lambda_r n_\mu^{(r)} \gamma^\mu\right) \psi(x) = 0, \quad r = a, b, \quad (7)$$

where  $\lambda_r = s\lambda_r^{(s)}$  take the values  $\pm 1$ . We will consider the FC in the region  $a \leq r \leq b$  where  $n_\mu^{(u)} = n_a \delta_\mu^1$ , with  $n_a = -1$  and  $n_b = 1$ . Note that the topology of the conical ring is nontrivial and the periodicity condition on the field should be specified along the  $\phi$ -direction as well. Here we impose a quasiperiodicity condition with a phase  $2\pi\chi$ :

$$\psi(t, r, \phi + \phi_0) = e^{2\pi i \chi} \psi(t, r, \phi). \quad (8)$$

The special cases include the untwisted and twisted fermionic fields with  $\chi = 0$  and  $\chi = 1/2$ , respectively. For the external gauge field we assume a simple form with the covariant components  $A_\mu = A\delta_\mu^2$  in the region  $a \leq r \leq b$ . The corresponding field strength  $F_{\mu\nu}$  vanishes on the conical ring and the effect of that configuration of gauge field on the properties of the fermionic vacuum is purely topological. Assuming that the 2D conical geometry under consideration is embedded in 3D Euclidean space, the parameter  $A$  can be interpreted in terms of the magnetic flux for a gauge field  $A'_k$ ,  $k = 0, 1, 2, 3$ , living in (3+1)-dimensional flat spacetime. Introducing 3D cylindrical coordinate system  $(\rho, \varphi, z)$  with the axis  $z$  along the axis of the cone, we get the relations  $\rho = r/q$  and  $\varphi = q\phi$ . If the magnetic field  $\mathbf{B} = \text{rot } \mathbf{A}$  corresponding to the vector potential  $A'_k$  is localized in the region  $\rho < a/q$  of the 3D space, then for the magnetic flux  $\Phi = \int \mathbf{B} \cdot d\mathbf{S}$ , threading the conical ring, one obtains  $\Phi = \oint \mathbf{A} \cdot d\mathbf{l} = 2\pi\rho A_\phi$ , where as an integration contour we have taken a circle on the conical ring and  $A_\phi$  is the physical azimuthal component of the vector potential. Now, by taking into account that  $A_\phi = -A/r$  and  $2\pi\rho = \phi_0 r$ , we find  $\Phi = -\phi_0 A$ . Note that in this interpretation we have a situation similar to that in braneworld models with extra dimensions: for a part of the fields the whole space is accessible (the gauge field in the problem at hand) and the another part of the fields (the fermion field) is confined to a hypersurface (the conical ring). As an example of physical realization of the 2D model embedded in 3D Euclidean space, in Section 4 we will consider graphene conical rings. The effect of the magnetic flux on the FC, discussed below, is of the Aharonov-Bohm-type and it does not depend on the profile of the magnetic field sourcing the flux. The spatial geometry of the problem under consideration with the magnetic flux is presented in Figure 1.

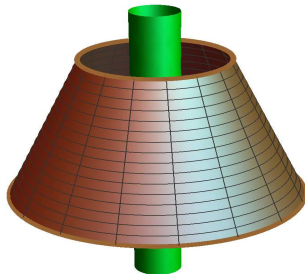


Figure 1: The geometry of a conical ring threaded by a magnetic flux.

The ground state FC is expressed in terms of the fermion two-point function  $S^{(1)}(x, x')$  as

$$\langle \bar{\psi}\psi \rangle = - \lim_{x' \rightarrow x} \text{Tr}(S^{(1)}(x, x')). \quad (9)$$

The two-point function describes the correlations of the vacuum fluctuations and is defined as the VEV  $S_{ik}^{(1)}(x, x') = \langle 0 | [\psi_i(x), \bar{\psi}_k(x')] | 0 \rangle$  with the spinor indices  $i$  and  $k$ . The trace in (9) is taken over those indices. The FC plays an important role in discussions of chiral symmetry breaking and dynamical mass generation for fermionic fields. Expanding the fermionic operator in terms of a complete set of the positive and negative energy mode functions  $\psi_\sigma^{(+)}$  and  $\psi_\sigma^{(-)}$ , obeying the conditions (7), (8),

and using the anticommutation relations for the fermionic annihilation and creation operators, the following mode sum is obtained for the FC

$$\langle \bar{\psi}\psi \rangle = -\frac{1}{2} \sum_{\sigma} \sum_{\kappa=-,+} \kappa \bar{\psi}_{\sigma}^{(\kappa)} \psi_{\sigma}^{(\kappa)}. \quad (10)$$

Here,  $\sigma$  stands for the complete set of quantum numbers specifying the solutions of the equation (6),  $\sum_{\sigma}$  is understood as a summation for discrete components and as an integration for continuous ones.

In the problem under consideration for the mode functions in the region  $a \leq r \leq b$  one has [59]

$$\psi_{\sigma}^{(\kappa)} = C_{\kappa} e^{iq(j+\chi)\phi - \kappa i E t} \left( \begin{array}{c} g_{\beta_j, \beta_j}(\gamma a, \gamma r) e^{-iq\phi/2} \\ \frac{\epsilon_j \gamma e^{iq\phi/2}}{\kappa E + sm} g_{\beta_j, \beta_j + \epsilon_j}(\gamma a, \gamma r) \end{array} \right), \quad (11)$$

where  $E = \sqrt{\gamma^2 + m^2}$  is the energy,  $j = \pm 1/2, \pm 3/2, \dots$ ,  $\epsilon_j = 1$  for  $j > -\alpha$  and  $\epsilon_j = -1$  for  $j < -\alpha$ ,

$$\beta_j = q|j + \alpha| - \epsilon_j/2. \quad (12)$$

Here and in what follows

$$\alpha = \chi + eA/q = \chi - e\Phi/(2\pi). \quad (13)$$

The radial functions in (11) are given by the expression

$$g_{\beta_j, \nu}(\gamma a, \gamma r) = Y_{\beta_j}^{(a)}(\gamma a) J_{\nu}(\gamma r) - J_{\beta_j}^{(a)}(\gamma a) Y_{\nu}(\gamma r), \quad (14)$$

with the Bessel and Neumann functions  $J_{\nu}(x)$ ,  $Y_{\nu}(\gamma r)$ , and with the notation

$$f_{\beta_j}^{(u)}(x) = \lambda_u n_u (\kappa \sqrt{x^2 + m_u^2} + sm_u) f_{\beta_j}(x) - \epsilon_j x f_{\beta_j + \epsilon_j}(x), \quad (15)$$

for  $f = J, Y$ ,  $u = a, b$ , and  $m_u = mu$ .

The mode functions (11) obey the boundary condition on the edge  $r = a$ . The eigenvalues of the radial quantum number  $\gamma$  are determined by the boundary condition on the edge  $r = b$ . They are solutions of the equation

$$C_{\beta_j}(b/a, \gamma a) \equiv J_{\beta_j}^{(a)}(\gamma a) Y_{\beta_j}^{(b)}(\gamma b) - J_{\beta_j}^{(b)}(\gamma b) Y_{\beta_j}^{(a)}(\gamma a) = 0. \quad (16)$$

We will denote by  $\gamma = \gamma_l$ ,  $l = 1, 2, \dots$ , the positive roots of this equation. The eigenvalues of  $\gamma$  are expressed as  $\gamma = \gamma_l = z_l/a$ . Note that under the change  $(\alpha, j) \rightarrow (-\alpha, -j)$  one has  $\beta_j \rightarrow \beta_j + \epsilon_j$  and  $\beta_j + \epsilon_j \rightarrow \beta_j$ . From here we can see that under the change

$$(\kappa, \alpha, j) \rightarrow (-\kappa, -\alpha, -j) \quad (17)$$

we get

$$f_{\beta_j}^{(u)}(u\gamma) \rightarrow -\epsilon_j (\lambda_u n_u / u) (\kappa E + sm) f_{\beta_j}^{(u)}(u\gamma), \quad (18)$$

and, hence, the roots  $\gamma_l$  are invariant under the transformation (17).

The normalization coefficient is given by

$$|C_{\kappa}|^2 = \frac{\pi q z}{16a^2} \frac{E + \kappa sm}{E} T_{\beta_j}^{ab}(z), \quad (19)$$

where  $z = z_l = \gamma_l a$ ,  $E = \sqrt{z^2/a^2 + m^2}$ , and we have defined the function

$$T_{\beta_j}^{ab}(z) = \frac{z}{E + \kappa sm} \left[ \frac{B_b J_{\beta_j}^{(a)2}(z)}{J_{\beta_j}^{(b)2}(zb/a)} - B_a \right]^{-1}, \quad (20)$$

with

$$B_u = u^2 \left[ E - \frac{\kappa \lambda_u n_u}{u} \left( \frac{E - \kappa s m}{2E} + \epsilon_j \beta_j \right) \right]. \quad (21)$$

Note that the parameters  $\chi$  and  $\Phi$  enter in the expression of the mode functions in the gauge-invariant combination  $\alpha$ . This shows that the phase  $\chi$  in the quasiperiodicity condition (8) is equivalent to a magnetic flux  $-2\pi\chi/e$  threading the ring and vice versa.

In addition to an infinite number of modes with  $\gamma = \gamma_l$ , depending on the boundary conditions, one can have a mode with  $\gamma a = i\eta$ ,  $\eta > 0$ . As it has been shown in [59], for that mode  $\eta \leq ma$  and, hence,  $E \geq 0$ . This means that under the boundary conditions (7) the vacuum state is always stable.

For half-integer values of the parameter  $\alpha$ , in addition to the modes with  $j \neq -\alpha$  and discussed above, a special mode with  $j = -\alpha$  is present. The upper and lower components of the corresponding mode functions are expressed in terms of the trigonometric functions. These mode functions and the equation determining the eigenvalues of the radial quantum number are given in [59]. For  $j = -\alpha$  and for boundary conditions with  $\lambda_b = -\lambda_a$ , one has also a zero energy mode with  $\gamma = im$ . In a way similar to that discussed in [59] for the vacuum expectation values of the charge and current densities, it can be seen that the special mode with  $j = -\alpha$  and  $E \neq 0$  does not contribute to the FC. The latter is a consequence of the cancellation of the contributions coming from the positive and negative energy modes. The contribution of the zero energy mode to the FC is zero as well. Note that the latter is not the case for the expectation values of the charge and current densities.

### 3 Fermion condensate

Given the complete set of fermionic modes, the FC on the conical ring is obtained by using the mode sum formula (10). First let us consider the case when all the roots of the eigenvalue equation are real. Substituting the mode functions (11), the FC in the region  $a \leq r \leq b$  is presented in the form

$$\langle \bar{\psi} \psi \rangle = -\frac{\pi q}{32a^2} \sum_j \sum_{\kappa=\pm} \sum_{l=1}^{\infty} T_{\beta_j}^{ab}(z) \frac{z}{E} \left[ (sm + \kappa E) g_{\beta_j, \beta_j}^2(z, zr/a) + (sm - \kappa E) g_{\beta_j, \beta_j + \epsilon_j}^2(z, zr/a) \right]_{z=z_l}, \quad (22)$$

where  $E = \sqrt{z^2/a^2 + m^2}$  and the summation goes over  $j = \pm 1/2, \pm 3/2, \dots$ . The operators  $\bar{\psi}$  and  $\psi$  in the left-hand side of (22) are taken at the same spacetime point and the expression on the right-hand side is divergent. Various regularization schemes can be used to make the expression finite. To be specific, we will assume that the regularization is done by introducing a cutoff function without writing it explicitly. The final result for the renormalized FC does not depend on the specific form of that function. By taking into account that the roots  $z_l$  are invariant under the transformation (17) and by using the transformation rule (18) we can see that the FC is an even periodic function of the parameter  $\alpha$ , defined by (13), with the period 1. In particular, we have periodicity with respect to the enclosed magnetic flux with the period equal to the flux quantum  $2\pi/e$ . If we present the parameter  $\alpha$  in the form  $\alpha = n_0 + \alpha_0$ , with  $|\alpha_0| \leq 1/2$  and  $n_0$  being an integer, then the FC will depend on the fractional part  $\alpha_0$  only. Note that the vacuum expectation values of the charge and current densities are odd periodic functions of the magnetic flux with the same period.

An alternative representation of the FC is obtained from (22) by using the Abel-Plana-type formula [90, 91]

$$\begin{aligned} \sum_{l=1}^{\infty} w(z_l) T_{\beta_j}^{ab}(z_l) &= \frac{4}{\pi^2} \int_0^{\infty} dx \frac{w(x)}{J_{\beta_j}^{(a)2}(x) + Y_{\beta_j}^{(a)2}(x)} - \frac{2}{\pi} \text{Res}_{z=0} \left[ \frac{w(z) H_{\beta_j}^{(1b)}(zb/a)}{C_{\beta_j}(b/a, z) H_{\beta_j}^{(1a)}(z)} \right] \\ &\quad - \frac{1}{\pi} \int_0^{\infty} dx \sum_{p=+,-} \frac{w(x e^{pi\pi/2}) K_{\beta_j}^{(bp)}(xb/a) / K_{\beta_j}^{(ap)}(x)}{K_{\beta_j}^{(ap)}(x) I_{\beta_j}^{(bp)}(xb/a) - I_{\beta_j}^{(ap)}(x) K_{\beta_j}^{(bp)}(xb/a)}. \end{aligned} \quad (23)$$

for the function  $w(z)$  analytic in the half-plane  $\text{Re } z > 0$  of the complex plane  $z$ . Here and below  $H_\nu^{(l)}(x)$ , with  $l = 1, 2$ , are the Hankel functions and the notation  $H_{\beta_j}^{(lu)}(x)$  is defined in accordance with (15). In the second integral on the right-hand side of (23), for the modified Bessel functions  $f_\nu(x) = I_\nu(x), K_\nu(x)$ , the notations

$$f_{\beta_j}^{(up)}(x) = \delta_f x f_{\beta_j + \epsilon_j}(x) + \lambda_u n_u \left[ \kappa \sqrt{(x e^{p\pi i/2})^2 + m_u^2} + s m_u \right] f_{\beta_j}(x), \quad (24)$$

are introduced with  $p = +, -, u = a, b$ , and

$$\delta_I = 1, \delta_K = -1. \quad (25)$$

Additional conditions on the function  $w(z)$  are given in [91]. By taking into account that

$$\sqrt{(x e^{p\pi i/2})^2 + m_u^2} = \begin{cases} \sqrt{m_u^2 - x^2}, & x < m_u, \\ p i \sqrt{x^2 - m_u^2}, & x > m_u, \end{cases} \quad (26)$$

for  $x \geq 0$ , we see that  $f_{\beta_j}^{(u+)}(x) = f_{\beta_j}^{(u-)}(x)$  in the range  $x \in [0, m_u]$ . In addition, for the function  $w(x)$  corresponding to the series over  $l$  in (22) one has  $w(x e^{-i\pi/2}) = -w(x e^{i\pi/2})$  for  $x \in [0, m_a]$ . From these properties it follows that for the FC the integrand of the last integral in (23) vanishes in the integration range  $x \in [0, m_a]$ . It can also be seen that for the FC the residue in (23) is zero.

As a result, applying the formula (23) for the series over  $l$  in (22), the FC in the region  $a \leq r \leq b$  is decomposed into two contributions. The first one, denoted below as  $\langle \bar{\psi} \psi \rangle_a$ , comes from the first term in the right-hand side of (23) and is presented in the form

$$\langle \bar{\psi} \psi \rangle_a = -\frac{q}{8\pi a^2} \sum_j \sum_{\kappa=\pm} \int_0^\infty dz \frac{z}{E} \frac{(sm + \kappa E) g_{\beta_j, \beta_j}^2(z, zr/a) + (sm - \kappa E) g_{\beta_j, \beta_j + \epsilon_j}^2(z, zr/a)}{J_{\beta_j}^{(a)2}(z) + Y_{\beta_j}^{(a)2}(z)}. \quad (27)$$

The second contribution comes from the last term in (23). Introducing the modified Bessel functions, we get the following representation of the FC:

$$\begin{aligned} \langle \bar{\psi} \psi \rangle &= \langle \bar{\psi} \psi \rangle_a + \frac{q}{2\pi^2} \sum_{n=0}^\infty \sum_{p=\pm 1} \int_m^\infty dx \frac{x}{\sqrt{x^2 - m^2}} \text{Re} \left\{ \frac{K_{n_p}^{(b)}(bx) / K_{n_p}^{(a)}(ax)}{G_{n_p}^{(ab)}(ax, bx)} \right. \\ &\quad \left. \times \left[ (sm + i\sqrt{x^2 - m^2}) G_{n_p, n_p}^{(a)2}(ax, rx) - (sm - i\sqrt{x^2 - m^2}) G_{n_p, n_p + 1}^{(a)2}(ax, rx) \right] \right\}, \quad (28) \end{aligned}$$

where instead of the summation over  $j$  we have introduced the summation over  $n$  with

$$n_p = q(n + 1/2 + p\alpha_0) - 1/2. \quad (29)$$

Here and in what follows, for the functions  $f_\nu(z) = I_\nu(z), K_\nu(z)$  we use the notation

$$f_{n_p}^{(u)}(z) = \delta_f z f_{n_p + 1}(z) + \lambda_u n_u (i\sqrt{z^2 - m_u^2} + s m_u) f_{n_p}(z), \quad (30)$$

with  $u = a, b$ , and the functions in the right-hand side of (28) are defined by

$$\begin{aligned} G_{n_p, \nu}^{(u)}(x, y) &= K_{n_p}^{(u)}(x) I_\nu(y) - (-1)^{\nu - n_p} I_{n_p}^{(u)}(x) K_\nu(y), \\ G_{n_p}^{(ab)}(x, y) &= K_{n_p}^{(a)}(x) I_{n_p}^{(b)}(y) - I_{n_p}^{(a)}(x) K_{n_p}^{(b)}(y). \end{aligned} \quad (31)$$

Similar to the case of the charge and current densities, discussed in [59], it can be shown that the expression (28) is valid in the presence of bound states as well. Under the replacements  $\lambda_u \rightarrow -\lambda_u$ ,  $s \rightarrow -s$  we have  $f_{n_p}^{(u)}(z) \rightarrow [f_{n_p}^{(u)}(z)]^*$  and the last term in (28) changes the sign.

The term  $\langle \bar{\psi}\psi \rangle_a$  in (28) does not depend on  $b$ . By using the asymptotic formulas for the modified Bessel functions (see, for example, [92]), it can be seen that in the limit  $b \rightarrow \infty$  the last term in (28) behaves as  $e^{-2mb}$  for a massive field and like  $(a/b)^{q(1-2|\alpha_0|)+1}$  for a massless field. From here it follows that  $\langle \bar{\psi}\psi \rangle_a = \lim_{b \rightarrow \infty} \langle \bar{\psi}\psi \rangle$  and the contribution  $\langle \bar{\psi}\psi \rangle_a$  presents the FC in the region  $a \leq r < \infty$  of (2+1)-dimensional conical spacetime for a fermionic field obeying the boundary condition (7) at  $r = a$ . Hence, the last term in (28) is interpreted as the contribution induced by the second boundary at  $r = b$  when we add it to the conical geometry with a single edge at  $r = a$ . In order to further extract the edge-induced contribution in  $\langle \bar{\psi}\psi \rangle_a$  we use the relation

$$\frac{g_{\beta_j, \nu}^2(z, y)}{J_{\beta_j}^{(a)2}(z) + Y_{\beta_j}^{(a)2}(z)} = J_{\nu}^2(y) - \sum_{l=1,2} \frac{J_{\beta_j}^{(a)}(z) H_{\nu}^{(l)2}(y)}{2H_{\beta_j}^{(l)2}(z)}. \quad (32)$$

where  $\nu = \beta_j, \beta_j + \epsilon_j$ . This relation is easily obtained by taking into account that  $J_{\beta_j}^{(a)2}(z) + Y_{\beta_j}^{(a)2}(z) = H_{\beta_j}^{(1a)}(z) H_{\beta_j}^{(2a)}(z)$ . Applying (32) for separate terms in (27), we can see that the part in the FC coming from the first term in the right-hand side of (32), denoted here by  $\langle \bar{\psi}\psi \rangle_0$ , does not depend on  $a$  and is presented as

$$\langle \bar{\psi}\psi \rangle_0 = -\frac{qsm}{4\pi} \sum_j \int_0^\infty dx x \frac{J_{\beta_j}^2(xr) + J_{\beta_j + \epsilon_j}^2(xr)}{\sqrt{x^2 + m^2}}. \quad (33)$$

This part corresponds to the FC in a boundary-free conical space and has been investigated in [74] for the case  $s = 1$ . The corresponding renormalized value is given by the expression

$$\begin{aligned} \langle \bar{\psi}\psi \rangle_{0, \text{ren}} = & -\frac{sm}{2\pi r} \left\{ \sum_{l=1}^{[q/2]} (-1)^l \frac{\cot(\pi l/q)}{e^{2mr} \sin(\pi l/q)} \cos(2\pi l \alpha_0) \right. \\ & \left. + \frac{q}{\pi} \sum_{\delta=\pm 1} \cos[q\pi(1/2 + \delta\alpha_0)] \int_0^\infty dy \frac{\tanh y}{e^{2mr} \cosh y} \frac{\sinh[q(1 - 2\delta\alpha_0)y]}{\cosh(2qy) - \cos(q\pi)} \right\}, \end{aligned} \quad (34)$$

where  $[q/2]$  is the integer part of  $q/2$ . Note that for points away from the edges of the conical ring the boundary-induced contribution in the FC is finite and the renormalization is required for the boundary-free part only.

The contribution to the FC  $\langle \bar{\psi}\psi \rangle_a$  coming from the last term in (32) is induced by the edge at  $r = a$  in the region  $a \leq r < \infty$ . That contribution is further transformed by rotating the integration contour over  $z$  by the angle  $\pi/2$  for the terms with the Hankel functions  $H_{\beta_j}^{(1)}(zr/a)$ ,  $H_{\beta_j + \epsilon_j}^{(1)}(zr/a)$ , and by the angle  $-\pi/2$  for the terms with the functions  $H_{\beta_j}^{(2)}(zr/a)$ ,  $H_{\beta_j + \epsilon_j}^{(2)}(zr/a)$ . The parts of the integrals over the intervals  $[0, ima]$  and  $[0, -ima]$  cancel each other. Introducing in the remaining integrals the modified Bessel functions the FC  $\langle \bar{\psi}\psi \rangle_a$  is presented in the form

$$\begin{aligned} \langle \bar{\psi}\psi \rangle_a = & \langle \bar{\psi}\psi \rangle_{0, \text{ren}} + \frac{q}{2\pi^2} \sum_{n=0}^{\infty} \sum_{p=\pm 1} \int_m^\infty dx \frac{x}{\sqrt{x^2 - m^2}} \text{Re} \left\{ \frac{I_{n_p}^{(a)}(ax)}{K_{n_p}^{(a)}(ax)} \right. \\ & \left. \times \left[ \left( sm + i\sqrt{x^2 - m^2} \right) K_{n_p}^2(rx) - \left( sm - i\sqrt{x^2 - m^2} \right) K_{n_p+1}^2(rx) \right] \right\}, \end{aligned} \quad (35)$$

where  $n_p$  is defined by (29). It can be seen that in the special case  $s = 1$ ,  $\lambda_a = 1$  this expression coincides with the result from [74]. The condensate given by (35) changes the sign under the replacement  $(s, \lambda_a) \rightarrow (-s, -\lambda_a)$ . Combining this property with the corresponding behaviour of the last term in (28), we conclude that the FC  $\langle \bar{\psi}\psi \rangle$  in the region  $a \leq r \leq b$  changes the sign under the transformation

$$(s, \lambda_a, \lambda_b) \rightarrow (-s, -\lambda_a, -\lambda_b). \quad (36)$$



For a massless field the FC in the boundary-free geometry vanishes and the single edge induced contribution is simplified to (see also [74] for the boundary condition with  $\lambda_a = 1$ )

$$\langle \bar{\psi}\psi \rangle_a = -\frac{\lambda_a q}{2\pi^2 a^2} \sum_{n=0}^{\infty} \sum_{p=\pm 1} \int_0^{\infty} dx \frac{K_{n_p}^2(xr/a) + K_{n_p+1}^2(xr/a)}{K_{n_p+1}^2(x) + K_{n_p}^2(x)}. \quad (37)$$

In this special case the total FC on a conical ring takes the form

$$\begin{aligned} \langle \bar{\psi}\psi \rangle &= \langle \bar{\psi}\psi \rangle_a - \frac{q}{2\pi^2} \sum_{n=0}^{\infty} \sum_{p=\pm 1} \int_0^{\infty} dx x \operatorname{Im} \left[ \frac{K_{n_p}^{(b)}(bx)}{K_{n_p}^{(a)}(ax)} \right. \\ &\quad \left. \times \frac{G_{n_p, n_p}^{(a)2}(ax, rx) + G_{n_p, n_p+1}^{(a)2}(ax, rx)}{G_{n_p}^{(ab)}(ax, bx)} \right], \end{aligned} \quad (38)$$

where now

$$f_{n_p}^{(u)}(z) = \delta_f z f_{n_p+1}(z) + i\lambda_u n_u z f_{n_p}(z). \quad (39)$$

Of course, for a massless field the FC does not depend on the parameter  $s$ . The zero FC for a massless field, realizing one of the irreducible representations of the Clifford algebra and propagating on a conical space without boundary, is related to the time-reversal ( $T$ -)symmetry of the model. The presence of the edges gives rise to nonzero FC and, hence, breaks the  $T$ -symmetry. This mechanism of  $T$ -symmetry breaking for planar fermionic systems have been discussed in [83]. The symmetry breaking was interpreted semiclassically in terms of the phases accumulated by the waves travelling along closed geodesics inside a bounded region and reflected from the boundary.

In the representation (28) for the FC on a conical ring with edges  $r = a$  and  $r = b$ , the part corresponding to a cut cone with  $a \leq r < \infty$  is explicitly separated. An alternative representation, where the part corresponding to a cone with finite radius  $b$  is extracted, is obtained from (28) using the identity

$$\begin{aligned} \frac{I_{n_p}^{(a)}(ax)}{K_{n_p}^{(a)}(ax)} K_{\nu}^2(y) + \frac{K_{n_p}^{(b)}(bx)}{K_{n_p}^{(a)}(ax)} \frac{G_{n_p, \nu}^{(a)2}(ax, y)}{G_{n_p}^{(ab)}(ax, bx)} \\ = \frac{K_{n_p}^{(b)}(bx)}{I_{n_p}^{(b)}(bx)} I_{\nu}^2(y) + \frac{I_{n_p}^{(a)}(ax)}{I_{n_p}^{(b)}(bx)} \frac{G_{n_p, \nu}^{(b)2}(bx, y)}{G_{n_p}^{(ab)}(ax, bx)}, \end{aligned} \quad (40)$$

with  $\nu = n_p, n_p + 1$ . Separating the contributions coming from the first term in the right-hand side, the FC in the region  $a \leq r \leq b$  is presented in the form

$$\begin{aligned} \langle \bar{\psi}\psi \rangle &= \langle \bar{\psi}\psi \rangle_b + \frac{q}{2\pi^2} \sum_{n=0}^{\infty} \sum_{p=\pm 1} \int_m^{\infty} dx \frac{x}{\sqrt{x^2 - m^2}} \operatorname{Re} \left\{ \frac{I_{n_p}^{(a)}(ax)/I_{n_p}^{(b)}(bx)}{G_{n_p}^{(ab)}(ax, bx)} \right. \\ &\quad \left. \times \left[ \left( sm + i\sqrt{x^2 - m^2} \right) G_{n_p, n_p}^{(b)2}(bx, rx) - \left( sm - i\sqrt{x^2 - m^2} \right) G_{n_p, n_p+1}^{(b)2}(bx, rx) \right] \right\}, \end{aligned} \quad (41)$$

where

$$\begin{aligned} \langle \bar{\psi}\psi \rangle_b &= \langle \bar{\psi}\psi \rangle_{0, \text{ren}} + \frac{q}{2\pi^2} \sum_{n=0}^{\infty} \sum_{p=\pm 1} \int_m^{\infty} dx \frac{x}{\sqrt{x^2 - m^2}} \operatorname{Re} \left\{ \frac{K_{n_p}^{(b)}(bx)}{I_{n_p}^{(b)}(bx)} \right. \\ &\quad \left. \times \left[ \left( sm + i\sqrt{x^2 - m^2} \right) I_{n_p}^2(rx) - \left( sm - i\sqrt{x^2 - m^2} \right) I_{n_p+1}^2(rx) \right] \right\}. \end{aligned} \quad (42)$$

In the limit  $a \rightarrow 0$  and for  $|\alpha_0| < 1/2$  the second term in the right-hand side of (41) tends to zero as  $a^{q(1-2|\alpha_0|)}$  whereas the first term does not depend on  $a$ . This allows to interpret the part  $\langle \bar{\psi}\psi \rangle_b$

as the FC on a cone  $0 \leq r \leq b$  for a field obeying the boundary condition (7) on a single circular boundary at  $r = b$ . With this interpretation, the last term in (41) corresponds to the contribution when we additionally add the boundary at  $r = a$  with the respective boundary condition from (7). In the special case  $s = 1$ ,  $\lambda_b = 1$  the FC (42) coincides with the result derived in [74].

For a massless field, from (41) we get the following alternative representation for the FC:

$$\begin{aligned} \langle \bar{\psi}\psi \rangle &= \langle \bar{\psi}\psi \rangle_b - \frac{q}{2\pi^2} \sum_{n=0}^{\infty} \sum_{p=\pm 1} \int_m^{\infty} dx x \operatorname{Im} \left[ \frac{I_{n_p}^{(a)}(ax)}{I_{n_p}^{(b)}(bx)} \right. \\ &\quad \left. \times \frac{G_{n_p, n_p}^{(b)2}(bx, rx) + G_{n_p, n_p+1}^{(b)2}(bx, rx)}{G_{n_p}^{(ab)}(ax, bx)} \right], \end{aligned} \quad (43)$$

with the single edge contribution

$$\langle \bar{\psi}\psi \rangle_b = -\frac{\lambda_b q}{2\pi^2 b^2} \sum_{n=0}^{\infty} \sum_{p=\pm 1} \int_0^{\infty} dx \frac{I_{n_p}^2(xr/b) + I_{n_p+1}^2(xr/b)}{I_{n_p}^2(x) + I_{n_p+1}^2(x)}. \quad (44)$$

The latter is negative for the boundary condition with  $\lambda_b = 1$  and positive for the condition with  $\lambda_b = -1$ .

The FC in (38) diverges on the edges  $r = a, b$ . The divergence at  $r = a$  comes from the single boundary part  $\langle \bar{\psi}\psi \rangle_a$  in the representation (28) and the divergence on the edge  $r = b$  comes from the term  $\langle \bar{\psi}\psi \rangle_b$  in (41). In order to find the leading term in the asymptotic expansion over the distance from the edge at  $r = u$ ,  $u = a, b$ , we note that for  $|r/u - 1| \ll 1$  the dominant contribution in the edge-induced parts  $\langle \bar{\psi}\psi \rangle_u$  (the last terms in (35) and (42)) come from large values of  $x$  and  $n$ . By using the uniform asymptotic expansions for the modified Bessel functions, to the leading order we get

$$\langle \bar{\psi}\psi \rangle \approx -\frac{\lambda_u}{8\pi(r-u)^2}. \quad (45)$$

In deriving this result we have additionally assumed that  $m|r-u| \ll 1$ . Near the edges the leading term does not depend on the mass, on the magnetic flux and on the angle deficit of the conical geometry. It is of interest to note that the vacuum expectation values of the charge and current densities are finite on the ring edges [59].

In Figure 2 we display the FC for a massless fermionic field on a conical ring as a function of the radial coordinate. The graphs are plotted for  $b/a = 8$ ,  $q = 1.5$  and  $\alpha_0 = 1/4$ . The curves I and II correspond to the boundary conditions on the edges with  $(\lambda_a, \lambda_b) = (1, 1)$  and  $(\lambda_a, \lambda_b) = (1, -1)$ , respectively. The graphs for the remaining combinations of the set  $(\lambda_a, \lambda_b)$  are obtained by taking into account the property that for a massless field the FC changes the sign under the replacement  $(\lambda_a, \lambda_b) \rightarrow (-\lambda_a, -\lambda_b)$ . In the case I the FC is negative everywhere. For the case II the condensate is negative near the edge  $r = a$  and positive near  $r = b$ . This behavior is in accordance with the asymptotic estimate (45).

The dependence of the FC on the parameter  $\alpha_0$  is depicted in Figure 3 for a massless field and for the parameters  $b/a = 8$  and  $q = 1.5$ . The full and dashed curves correspond to  $r/a = 3$  and  $r/a = 5$ . As in Figure 2, the graphs I and II are for the sets  $(\lambda_a, \lambda_b) = (1, 1)$  and  $(\lambda_a, \lambda_b) = (1, -1)$ , respectively. The FC is continuous at half-integer values of the ratio of the magnetic flux to the flux quantum. The corresponding derivative for the case  $(\lambda_a, \lambda_b) = (1, 1)$  is continuous as well. For the boundary conditions with  $(\lambda_a, \lambda_b) = (1, -1)$  the derivative of the FC with respect to the magnetic flux is discontinuous for half-integer values of the ratio of the magnetic flux to the flux quantum.

Figure 4 displays the FC as a function of the parameter  $q$ , determining the planar angle deficit for conical geometry. The graphs are plotted for a massless field and for the values of the parameters

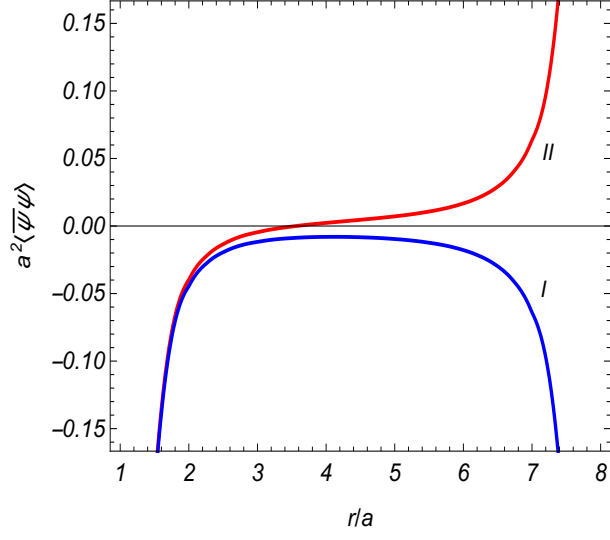


Figure 2: The radial dependence of the FC for a massless field on a conical ring with the parameters  $b/a = 8$ ,  $q = 1.5$ ,  $\alpha_0 = 1/4$ . The graphs I and II correspond to the sets  $(\lambda_a, \lambda_b) = (1, 1)$  and  $(\lambda_a, \lambda_b) = (1, -1)$ , respectively.

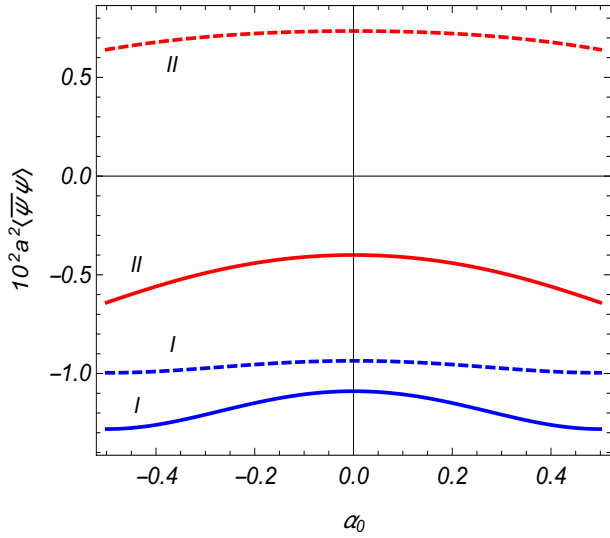


Figure 3: The FC versus the parameter  $\alpha_0$  for a massless field. The graphs are plotted for  $b/a = 8$ ,  $q = 1.5$ ,  $r/a = 3$  (full curves) and  $r/a = 5$  (dashed curves).

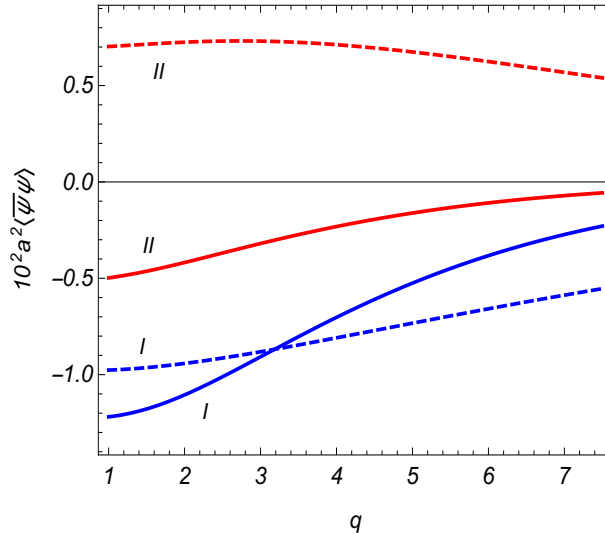


Figure 4: The dependence of the FC on the planar angle deficit of the conical space for  $\alpha_0 = 1/4$ . The values of the remaining parameters are the same as those for Figure 3.

$b/a = 8$ ,  $\alpha_0 = 1/4$ ,  $r/a = 3$  (full curves) and  $r/a = 5$  (dashed curves). As before, the curves I and II correspond to  $(\lambda_a, \lambda_b) = (1, 1)$  and  $(\lambda_a, \lambda_b) = (1, -1)$ , respectively.

All the graphs above were plotted for a massless field. In order to see the effects of finite mass, in Figure 5 we depicted the dependence of the FC on the dimensionless parameter  $ma$  for  $s = 1$ ,  $b/a = 8$ ,  $q = 1.5$ ,  $r/a = 2$  and  $\alpha_0 = 1/4$ . The curves I,II,III,IV correspond to the sets of discrete parameters  $(\lambda_a, \lambda_b) = (1, 1)$ ,  $(1, -1)$ ,  $(-1, 1)$  and  $(-1, -1)$ , respectively. The graphs for  $s = -1$  are obtained from those in Figure 5 by taking into account that the FC changes the sign under the transformation (36). As seen, the dependence on the mass, in general, is not monotonic. Of course, as we could expect the FC tends to zero for large values of the mass.

In the discussion above we have considered the simplest configuration of external gauge field which can be interpreted in terms of the magnetic flux threading the conical ring. The magnetic field is zero on the ring, where the fermion field is localized, and its influence is purely topological. New interesting effects in (2+1)-dimensional fermionic models appear in the presence of magnetic fields directly interacting with fermions. In particular, the formation of the FC and chiral symmetry breaking have been studied extensively in the literature (for a recent review see [93]). These investigations have been done within the framework of models with four-fermion and/or gauge interactions. They have demonstrated that magnetic fields serve as a catalyst of chiral symmetry breaking and the latter occurs even in the limit of weak gauge couplings. In some models the FC is related to the gauge field condensate  $\langle F_{\mu\nu} F^{\mu\nu} \rangle$ . An example is the relation  $\langle \bar{\psi} \psi \rangle \sim -\langle F_{\mu\nu} F^{\mu\nu} \rangle / m_\psi$  ( $F_{\mu\nu}$  is the gluon field strength tensor and  $m_\psi$  is the mass of the  $\psi$ -quark) between the quark and gluon condensates in quantum chromodynamics, valid in the heavy quark limit [94]. This relation gives the leading order term in the expansion over  $1/m_\psi$ . The gauge field condensate can also be formed for abelian gauge fields (see, for example, [95] for the formation of photon condensate in braneworld models on the AdS bulk).

As it has been mentioned before, in the model under consideration with boundary conditions (7) for the eigenvalues of the radial quantum number one has  $\gamma^2 + m^2 > 0$  and the vacuum state is stable. However, the inclusion of fermion interactions may lead to instabilities, as a result of which phase transitions take place. The FC appears as an order parameter in those transitions. In particular, the phase transitions, the chiral symmetry breaking and dynamical mass generation within the framework of (2+1)-dimensional Nambu–Jona-Lasinio (NJL) (or Gross-Neveu)-type models with four-fermion

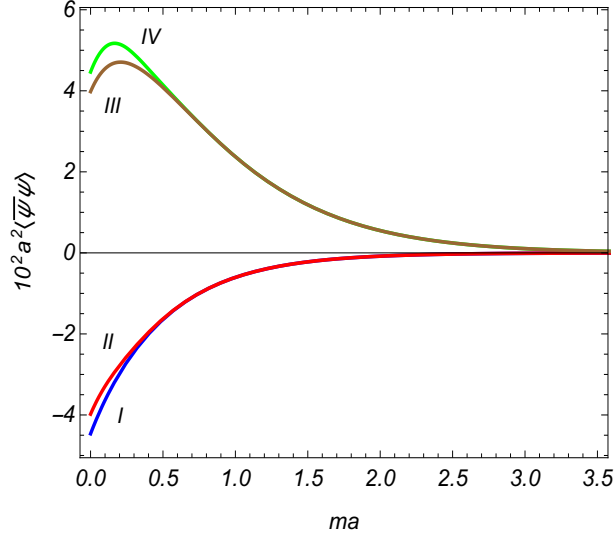


Figure 5: The FC as a function of the mass for  $s = 1$  and for fixed values  $b/a = 8$ ,  $q = 1.5$ ,  $r/a = 2$ ,  $\alpha_0 = 1/4$ . The separate graphs correspond to different combinations of the boundary conditions on the ring edges.

interactions have been previously discussed in the literature (see, for example, [93, 96, 97, 98, 99, 100] and the references [101, 102, 103] for applications in graphene). The influence of additional boundary conditions on the fermionic field, induced by the presence of boundaries or by compactification of spatial dimensions, was investigated as well (see, for instance, [41, 43, 104, 105, 106, 107, 108] and references therein). In particular, it has been shown that those conditions may either reduce or enlarge the chiral breaking region. In some cases the compactification may exclude the possibility for the dynamical symmetry breaking.

## 4 Fermion condensate in P- and T-symmetric models

For a fermion field  $\psi(x)$  in two spatial dimensions, realizing one of the irreducible representations of the Clifford algebra, the term  $m\bar{\psi}\psi$  in the corresponding Lagrangian density is not invariant with respect to the parity ( $P$ ) and time-reversal ( $T$ ) transformations. The  $P$ - and  $T$ -symmetries can be restored considering models involving two fields  $\psi_{(+1)}$  and  $\psi_{(-1)}$  realizing inequivalent irreducible representations and having the same mass. The corresponding Lagrangian density is given by  $L = \sum_{s=\pm 1} L_{(s)}$  with the separate terms from (3). We assume that the fields obey the boundary conditions (5) on the ring edges. The total FC is presented in two equivalent forms,  $\sum_{s=\pm 1} \langle \bar{\psi}_{(s)} \psi_{(s)} \rangle$  and  $\sum_{s=\pm 1} \langle \bar{\psi}'_{(s)} \psi'_{(s)} \rangle$ . An equivalent representation of the model is obtained combining the two-component fields in a single 4-component spinor  $\Psi = (\psi_{(+1)}, \psi_{(-1)})^T$  with the Lagrangian density

$$L = \bar{\Psi} (i\gamma_{(4)}^\mu D_\mu - m) \Psi, \quad (46)$$

where the  $4 \times 4$  Dirac matrices are given by  $\gamma_{(4)}^\mu = I \otimes \gamma^\mu$  for  $\mu = 0, 1$ , and  $\gamma_{(4)}^2 = \sigma_3 \otimes \gamma^2$  with  $\sigma_3$  being the Pauli matrix. For the corresponding FC one has the standard expression  $\langle \bar{\Psi}(x) \Psi(x) \rangle$ . The boundary conditions on the edges  $r = a, b$  are rewritten as

$$\left(1 + i\Lambda_r n_\mu \gamma_{(4)}^\mu\right) \Psi(x) = 0, \quad (47)$$

with  $\Lambda_r = \text{diag}(\lambda_r^{(+1)}, \lambda_r^{(-1)})$ . Alternatively, we can introduce the spinor  $\Psi' = (\psi'_{(+1)}, \psi'_{(-1)})^T$  and the set of gamma matrices  $\gamma'_{(4)}^\mu = \sigma_3 \otimes \gamma^\mu$ . For the corresponding Lagrangian density one gets

$L = \bar{\Psi}'(i\gamma_{(4)}^{\mu} D_{\mu} - m)\Psi'$  and for the FC  $\langle \bar{\Psi}'(x)\Psi'(x) \rangle$ . Now the boundary conditions take the form  $(1 + i\Lambda_r n_{\mu} \gamma_{(4)}^{\mu}) \Psi'(x) = 0$ . The latter has the same form as (47), though with different representation of the gamma matrices.

Note that by adding to the set of the gamma matrices  $\gamma_{(4)}^{\mu}$ ,  $\mu = 0, 1, 2$ , the Dirac matrix  $\gamma_{(4)}^3$  we get the set  $\gamma_{(4)}^{\mu}$ ,  $\mu = 0, 1, 2, 3$ , that obeys the Clifford algebra in (3+1)-dimensional spacetime. Now we can construct the chiral  $\gamma_{(4)}^5 = i \prod_{\mu=0}^3 \gamma_{(4)}^{\mu}$  matrix which anticommutes with the  $\gamma_{(4)}^{\mu}$ ,  $\mu = 0, 1, 2, 3$ , matrices and realizes the chiral transformation  $\Psi_{\text{ch}}(x) \rightarrow e^{i\chi_{\text{ch}} \gamma_{(4)}^5} \Psi(x)$  with a phase  $\chi_{\text{ch}}$ . For a massless field the Lagrangian density (46) is invariant under the chiral transformation but the boundary condition (47) is not. In the literature bag models for hadrons have been considered with boundary conditions invariant under the chiral transformation (chiral bag models, for reviews see [109, 110, 111]). In those models the chiral symmetry is restored by introducing a chiral field that is coupled with the quarks at the bag surface. The chiral field can be expressed in terms of the isovector pion field. In chiral bag models the boundary condition on the fermionic field at the bag surface has the form  $(e^{iw\gamma_{(4)}^5} + in_{\mu} \gamma_{(4)}^{\mu}) \Psi(x) = 0$ , where the coefficient  $w$  in the exponent is expressed through the pion field on the bag surface.

Let us consider different combinations of the boundary conditions for the fields  $\psi_{(+1)}$  and  $\psi_{(-1)}$ . First we assume that  $\lambda_u^{(+1)} = \lambda_u^{(-1)}$ ,  $u = a, b$ . For the coefficients in the boundary conditions for the fields  $\psi'_{(+1)}$  and  $\psi'_{(-1)}$  one gets  $\lambda_u^{(-1)'} = -\lambda_u^{(+1)'}$ . From here we conclude that the condensates  $\langle \bar{\psi}_{(+1)} \psi_{(+1)} \rangle$  and  $\langle \bar{\psi}_{(-1)} \psi_{(-1)} \rangle$  are obtained from the formulas in the previous sections taking  $s = 1$ ,  $\lambda_u = \lambda_u^{(+1)}$  and  $s = -1$ ,  $\lambda_u = -\lambda_u^{(+1)}$ , respectively. If the parameter  $\chi$  in the condition (8) and the charges  $e$  are the same for the fields  $\psi_{(+1)}$  and  $\psi_{(-1)}$ , then the parameter  $\alpha$  is the same as well. Now, recalling that the FC discussed in the previous section, changes the sign under the replacement  $(s, \lambda_u) \rightarrow (-s, -\lambda_u)$ , we see that the total fermionic condensate vanishes. This means that in the model at hand with two fields and with the parameters in the boundary conditions  $\lambda_u^{(+1)} = \lambda_u^{(-1)}$  the Casimir contributions induced by the edges do not break the parity and time-reversal symmetries. In the second case with  $\lambda_u^{(+1)} = -\lambda_u^{(-1)}$ , the fields  $\psi_{(+1)}$  and  $\psi_{(-1)}$  obey different boundary conditions, whereas for the fields  $\psi'_{(+1)}$  and  $\psi'_{(-1)}$  the boundary conditions are the same. In this case the total FC is nonzero and the parity and time-reversal symmetries are broken by the boundary conditions. Note that, the nonzero FC may appear in the first case as well if the masses or the phases  $\chi$  for separate fields are different. Hence, the edge-induced effects provide a mechanism for time-reversal symmetry breaking in the absence of magnetic fields.

Among the interesting condensed matter realizations of fermionic models in (2+1)-dimensional spacetime is graphene. For a given spin degree of freedom, the effective description of the long-wavelength properties of the electronic subsystem is formulated in terms of 4-component fermionic field

$$\Psi = (\psi_{+,A}, \psi_{+,B}, \psi_{-,A}, \psi_{-,B})^T. \quad (48)$$

Two 2-component spinors  $\psi_+ = (\psi_{+,AS}, \psi_{+,BS})$  and  $\psi_- = (\psi_{-,AS}, \psi_{-,BS})$  correspond to two inequivalent points  $\mathbf{K}_+$  and  $\mathbf{K}_-$  at the corners of the hexagonal Brillouin zone for the graphene lattice. The components  $\psi_{\pm,A}$  and  $\psi_{\pm,B}$  present the amplitude of the electron wave function on the triangular sublattices  $A$  and  $B$ . The Lagrangian density for the field  $\Psi$  is given as (in standard units)

$$L_g = \bar{\Psi} [i\hbar\gamma_{(4)}^0 \partial_t + i\hbar v_F \sum_{l=1,2} \gamma_{(4)}^l (\nabla_l + ieA_l/\hbar c) - \Delta] \Psi, \quad (49)$$

where  $c$  is the speed of light,  $v_F \approx 7.9 \times 10^7$  cm/s is the Fermi velocity, and  $\Delta$  is the energy gap in the spectrum. The spatial components of the covariant derivative are expressed as  $D_l = \nabla_l + ieA_l/\hbar c$  with  $e$  being the electron charge. Various mechanisms for the generation of the gap, with the range  $1 \text{ meV} \lesssim \Delta \lesssim 1 \text{ eV}$ , have been considered in the literature. For the corresponding Dirac mass and the

related Compton wavelength one has  $m = \Delta/v_F^2$  and  $a_C = \hbar v_F/\Delta$ . The characteristic energy scale in graphene made structures is given by  $\hbar v_F/a_0 \approx 2.51$  eV, where  $a_0$  is the inter-atomic distance for the graphene lattice. The fields  $\psi_+$  and  $\psi_-$  correspond to the fields  $\psi_{(+1)}$  and  $\psi_{(-1)}$  in our consideration above and the Lagrangian density (49) is the analog of (46). Hence, the parameter  $s$  corresponds to the valley-indices  $+$  and  $-$  in graphene physics.

For graphitic cones the allowed values of the opening angle are given by  $\phi_0 = 2\pi(1 - n_c/6)$ , where  $n_c = 1, 2, \dots, 5$ . The transformation properties of the spinor fields under the rotation by the angle  $\phi_0$  about the cone axis are studied in [63, 65, 67, 70]. For odd values of  $n_c$  the condition that relates the spinors with the arguments  $\phi + \phi_0$  and  $\phi$  mixes the valley indices by the matrix  $e^{-i\pi n_c \tau_2/2}$  with the Pauli matrix  $\tau_2$  acting on those indices. One can diagonalize the corresponding quasiperiodicity condition by a unitary transformation. For graphitic cones with even  $n_c$  the components with different values of the valley-index are not mixed by the quasiperiodicity condition. The latter corresponds to (8) with the inequivalent values  $\chi = \pm 1/3$  for the parameter  $\chi$ . In accordance with the consideration given above, if the boundary conditions and the masses for the fields corresponding to different valleys are the same, the contributions to the FC coming from those fields cancel each other and the total FC vanishes. However, some mechanisms for the gap generation in the spectrum break the valley symmetry (an example is the chemical doping) and the corresponding Dirac masses for the fields  $\psi_+$  and  $\psi_-$  differ. In this case one has no cancellation and a nonzero total FC is formed. As it has been mentioned above, the nonzero FC is also generated by imposing different boundary conditions on the edges of the ring for the fields corresponding to different valleys. In these cases the expression of the FC for a given spin degree of freedom is obtained by combining the formulas given above for separate contributions coming from different valleys. In the corresponding expressions it is convenient to introduce the Compton wavelengths  $a_{C+}$  and  $a_{C-}$  instead of the Dirac masses  $m_+$  and  $m_-$  through the replacements  $m_{\pm}u \rightarrow u/a_{C\pm}$  for  $u = a, b, r$ .

The boundary conditions for fermions in the effective description of graphene structures with edges (graphene nanoribbons) depend on the atomic terminations. For special cases of zigzag and armchair edges those conditions have been discussed in [85] (for a generalization see [89]). The equivalence between the boundary conditions considered in [83] and [85] has been discussed in [89]. The boundary conditions for more general types of the atomic terminations in graphene sheets were studied in [84, 86, 89]. The general boundary conditions contain four parameters.

## 5 Conclusion

The FC is an important characteristic of fermionic fields that plays an important role in discussions of chiral symmetry breaking and dynamical generation of mass. It appears as an order parameter for the confinement-deconfinement phase transitions. In the present paper we have investigated the FC for a (2+1)-dimensional fermionic field localized on a conical ring with a general value of the planar angle deficit. The consideration is presented for both inequivalent irreducible representations of the Clifford algebra. The boundary conditions on the edges of the ring are taken in the form (7) with discrete parameters  $\lambda_a$  and  $\lambda_b$ . As a special case they include the boundary condition used in MIT bag model of hadrons for confinement of quarks. The mode-sum for the FC contains summation over the eigenvalues of the radial quantum number  $\gamma$ . The latter are determined from the boundary conditions on the ring edges and are roots of the transcendental equation (16). Depending on the values of the discrete parameters  $(s, \lambda_a, \lambda_b)$ , one can have modes with purely imaginary values of  $\gamma$ . For those modes, corresponding to bound states, we have  $\gamma^2 + m^2 \geq 0$ . This shows that for boundary conditions under consideration the fermionic vacuum state is always stable.

For an equivalent representation of the FC, we have applied the generalized Abel-Plana-type formula (23) to the series over the eigenvalues of  $\gamma$ . That allowed to extract explicitly the part in the FC corresponding to the region  $a \leq r < \infty$  of a conical space with a single adge and to present the part induced by the second edge in the form of the integral that is well adapted for numerical evaluations

(last term in (28)). The first contribution, corresponding to the conical region  $a \leq r < \infty$  (the second edge at  $r = b$  is absent), is further decomposed in the form of the sum of the boundary-free and edge-induced terms (formula (35)). An alternative representation of the FC on a conical ring, given by (41), is obtained by using the identity (40) for the modified Bessel functions. In that representation the part in the FC is extracted which corresponds to a finite radius cone (with the radius  $b$ ) and the last term in (41) is induced by the second edge at  $r = a$ , added to that geometry. For a massless field the boundary-free contribution in the FC vanishes and the nonzero FC is entirely due to the presence of boundaries (due to the Casimir effect). In this case the expressions for the edge-induced contributions to the FC are simplified to (38) and (43) with the single-edge geometry parts (37) and (44). The latter are positive for the boundary condition with  $\lambda_u < 0$  and negative for  $\lambda_u > 0$ .

All the separate contributions to the FC on the conical ring are even periodic functions of the magnetic flux, enclosed by the ring, with the period equal to the flux quantum. At small distances from the edge at  $r = u$ ,  $u = a, b$ , the leading term in the asymptotic expansion over the distance is given by the simple expression (45). The leading term does not depend on the mass and on the magnetic flux and is positive (negative) for the boundary condition with  $\lambda_u < 0$  ( $\lambda_u > 0$ ). For a massless field the FC in the boundary-free conical geometry vanishes and the nonzero contributions are purely edge-induced effects. This provides a mechanism for  $T$ -symmetry breaking in the absence of magnetic fields.

For a fermionic field realizing one of the irreducible representations of the Clifford algebra, the mass term in the Lagrangian density is not invariant under the parity and time-reversal transformations. Invariant fermionic models are constructed combining two fields corresponding to two inequivalent irreducible representations. In those models, the total FC is obtained by summing the contributions coming from the separate fields. The latter are obtained based on the results presented in section 3. If the parameters  $(\chi, \lambda_u)$  and the masses for the separate fields are the same, then the corresponding contributions cancel each other and the total FC is zero. In this case the Casimir-type contributions do not break the parity and time-reversal symmetries of the model. If at least one of the parameters  $(\chi, \lambda_u, m)$  is different for the fields in the combined Lagrangian, the total FC is nonzero and the symmetries are broken. The results obtained in the paper can be applied for the investigation of the FC in graphitic cones with circular edges. The opening angle of the latter can be used as an additional parameter to control the electronic properties. In the long-wavelength approximation these properties are well described by the Dirac model with appropriate periodicity conditions with respect to the rotations around the cone axis.

## Acknowledgments

A.A.S. was supported by the grant No. 20RF-059 of the Committee of Science of the Ministry of Education, Science, Culture and Sport RA, and by the "Faculty Research Funding Program" (PMI Science and Enterprise Incubator Foundation). T.A.P. was supported by the grant No. 20AA-1C005 of the Committee of Science of the Ministry of Education, Science, Culture and Sport RA, and by the "Faculty Research Funding Program" (PMI Science and Enterprise Incubator Foundation).

## References

- [1] Fradkin, E. *Field Theories of Condensed Matter Physics*; Cambridge University Press: Cambridge, UK, 2013.
- [2] Marino, E.C. *Quantum Field Theory Approach to Condensed Matter Physics*; Cambridge University Press: Cambridge, UK, 2017.



- [3] Gusynin, V.P.; Sharapov, S.G.; Carbotte, J.P. AC Conductivity of Graphene: from Tight-Binding Model to 2+1-Dimensional Quantum Electrodynamics. *Int. J. Mod. Phys. B* **2007**, *21*, 4611. DOI:10.1142/S0217979207038022.
- [4] Castro Neto, A.H.; Guinea, F.; Peres, N.M.R.; Novoselov, K.S.; Geim, A.K. The electronic properties of graphene. *Rev. Mod. Phys.* **2009**, *81*, 109. DOI:10.1103/RevModPhys.81.109.
- [5] Qi, X.-L.; Zhang, S.-C. Topological insulators and superconductors. *Rev. Mod. Phys.* **2011**, *83*, 1057. DOI:10.1103/RevModPhys.83.1057.
- [6] Mostepanenko, V.M.; Trunov, N.N. *The Casimir Effect and its Applications*; Clarendon Press: Oxford, UK, 1997.
- [7] Elizalde, E.; Odintsov, S.D.; Romeo, A.; Bytsenko, A.A.; Zerbini, S. *Zeta Regularization Techniques with Applications*; World Scientific: Singapore, 1994.
- [8] Milton, K.A. *The Casimir Effect: Physical Manifestation of Zero-Point Energy*; World Scientific: Singapore, 2002.
- [9] Bordag, M.; Klimchitskaya, G.L.; Mohideen, U.; Mostepanenko, V.M. *Advances in the Casimir Effect*; Oxford University Press: New York, USA, 2009.
- [10] Dalvit, D.; Milonni, P.; Roberts, D.; da Rosa, F., Eds. *Casimir Physics*, Lecture Notes in Physics; Vol. 834, Springer-Verlag: Berlin, Germany, 2011.
- [11] Bordag, M.; Fialkovsky, I.V.; Gitman, D.M.; Vassilevich, D.V. Casimir interaction between a perfect conductor and graphene described by the Dirac model. *Phys. Rev. B* **2009**, *80*, 245406. DOI:10.1103/PhysRevB.80.245406.
- [12] Gómez-Santos, G. Thermal van der Waals interaction between graphene layers. *Phys. Rev. B* **2009**, *80*, 245424. DOI:10.1103/PhysRevB.80.245424.
- [13] Drosdoff, D.; Woods, L.M. Casimir forces and graphene sheets. *Phys. Rev. B* **2010**, *82*, 155459. DOI:10.1103/PhysRevB.82.155459.
- [14] Fialkovsky, I.V.; Marachevsky, V.N.; Vassilevich, D.V. Finite-temperature Casimir effect for graphene. *Phys. Rev. B* **2011**, *84*, 035446. DOI:10.1103/PhysRevB.84.035446.
- [15] Sernelius, B.E. Casimir interactions in graphene systems. *Europhys. Lett.* **2011**, *95*, 57003. DOI:10.1209/0295-5075/95/57003.
- [16] Phan, A.D.; Woods, L.M.; Drosdoff, D.; Bondarev, I.V.; Viet, N.A. Temperature dependent graphene suspension due to thermal Casimir interaction. *Appl. Phys. Lett.* **2012**, *101*, 113118. DOI:10.1063/1.4752745.
- [17] Chaichian, M.; Klimchitskaya, G.L.; Mostepanenko, V.M.; Tureanu, A. Thermal Casimir-Polder interaction of different atoms with graphene. *Phys. Rev. A* **2012**, *86*, 012515. DOI:10.1103/PhysRevA.86.012515.
- [18] Bordag, M.; Klimchitskaya, G.L.; Mostepanenko, V.M. Thermal Casimir effect in the interaction of graphene with dielectrics and metals. *Phys. Rev. B* **2012**, *86*, 165429. DOI:10.1103/PhysRevB.86.165429.
- [19] Sernelius, B.E. Retarded interactions in graphene systems. *Phys. Rev. B* **2012**, *85*, 195427. DOI:10.1103/PhysRevB.85.195427.

- [20] Klimchitskaya, G.L.; Mostepanenko, V.M. Van der Waals and Casimir interactions between two graphene sheets. *Phys. Rev. B* **2013**, *87*, 075439. DOI:10.1103/PhysRevB.87.075439.
- [21] Phan, A.D.; Phan, T. Casimir interactions in strained graphene systems. *Phys. Status Solid RRL* **2014**, *8*, 1003. DOI:10.1002/pssr.201409421.
- [22] Klimchitskaya, G.L.; Mohideen, U.; Mostepanenko, V.M. Theory of the Casimir interaction from graphene-coated substrates using the polarization tensor and comparison with experiment. *Phys. Rev. B* **2014**, *89*, 115419. DOI:10.1103/PhysRevB.89.115419.
- [23] Dobson, J.F.; Gould, T.; Vignale, G. How Many-Body Effects Modify the van der Waals Interaction between Graphene Sheets. *Phys. Rev. X* **2014**, *4*, 021040. DOI:10.1103/PhysRevX.4.021040.
- [24] Bordag, M.; Klimchitskaya, G.L.; Mostepanenko, V.M.; Petrov, V.M. Quantum field theoretical description for the reflectivity of graphene. *Phys. Rev. D* **2015**, *91*, 045037. DOI:10.1103/PhysRevD.91.045037.
- [25] Sernelius, B.E. Casimir effects in systems containing 2D layers such as graphene and 2D electron gases. *J. Phys.: Condens. Matter* **2015**, *27*, 214017. DOI:10.1088/0953-8984/27/21/214017.
- [26] Bordag, M.; Klimchitskaya, G.L.; Mostepanenko, V.M.; Petrov, V.M. Quantum field theoretical description for the reflectivity of graphene. *Phys. Rev. D* **2016**, *93*, 089907(E). DOI:10.1103/PhysRevD.93.089907.
- [27] Khusnutdinov, N.; Kashapov, R.; Woods, L.M. Casimir-Polder effect for a stack of conductive planes. *Phys. Rev. A* **2016**, *94*, 012513. DOI:10.1103/PhysRevA.94.012513.
- [28] Drosdoff, D.; Bondarev, I.V.; Widom, A.; Podgornik, R.; Woods, L.M. Charge-Induced Fluctuation Forces in Graphitic Nanostructures. *Phys. Rev. X* **2016**, *6*, 011004. DOI:10.1103/PhysRevX.6.011004.
- [29] Inui, N. Casimir effect on graphene resonator. *J. Appl. Phys.* **2016**, *119*, 104502. DOI:10.1063/1.4943588.
- [30] Bimonte, G.; Klimchitskaya, G.L.; Mostepanenko, V.M. How to observe the giant thermal effect in the Casimir force for graphene systems. *Phys. Rev. A* **2017**, *96*, 012517. DOI:10.1103/PhysRevA.96.012517.
- [31] Bordag, M.; Fialkovsky, I.; Vassilevich, D. Casimir interaction of strained graphene. *Phys. Lett. A* **2017**, *381*, 2439. DOI:10.1016/j.physleta.2017.05.040.
- [32] Martinez, J.C.; Chen, X.; Jalil, M.B.A. Casimir effect and graphene: Tunability, scalability, Casimir rotor. *AIP Advances* **2018**, *8*, 015330. DOI:10.1063/1.5007787.
- [33] Derras-Chouk, A.; Chudnovsky, E.M.; Garanin, D.A.; Jaafar, R. Graphene cantilever under Casimir force. *J. Phys. D: Appl. Phys.* **2018**, *51*, 195301. DOI:10.1088/1361-6463/aaba6a.
- [34] Khusnutdinov, N.; Woods, L.M. Casimir Effects in 2D Dirac Materials (Scientific Summary). *JETP Lett.* **2019**, *110*, 183. DOI:10.1134/S0021364019150013.
- [35] Klimchitskaya, G.L.; Mohideen, U.; Mostepanenko, V.M. The Casimir force between real materials: Experiment and theory. *Rev. Mod. Phys.* **2009**, *81*, 1827. DOI:10.1103/RevModPhys.81.1827.
- [36] Woods, L.M.; Dalvit, D.A.R.; Tkatchenko, A.; Rodriguez-Lopez, P.; Rodriguez, A.W.; Podgornik, R. Materials perspective on Casimir and van der Waals interactions. *Rev. Mod. Phys.* **2016**, *88*, 045003. DOI:10.1103/RevModPhys.88.045003.

- [37] Klimchitskaya, G.L.; Mostepanenko, V.M. Casimir and Casimir-Polder forces in graphene systems: Quantum field theoretical description and thermodynamics. *Universe* **2020**, *6*, 150. DOI:10.3390/universe6090150.
- [38] Rodriguez-Lopez, P.; Kort-Kamp, W.J.M.; Dalvit, D.A.R.; Woods, L.M. Casimir force phase transitions in the graphene family. *Nat. Commun.* **2017**, *8*, 14699. DOI:10.1038/ncomms14699.
- [39] Elizalde, E.; Leseduardte, S.; Odintsov, S.D. Chiral symmetry breaking in the Nambu-Jona-Lasinio model in curved spacetime with a nontrivial topology. *Phys. Rev. D* **1994**, *49*, 5551. DOI:10.1103/PhysRevD.49.5551.
- [40] Inagaki, T.; Muta, T.; Odintsov, S.D. Dynamical Symmetry Breaking in Curved Spacetime. *Prog. Theor. Phys. Suppl.* **1997**, *127*, 93. DOI:10.1143/PTP.127.93.
- [41] Flachi, A. Interacting fermions, boundaries, and finite size effects. *Phys. Rev. D* **2012**, *86*, 104047. DOI:10.1103/PhysRevD.86.104047.
- [42] Flachi, A. Dual fermion condensates in curved space. *Phys. Rev. D* **2013**, *88*, 085011. DOI:10.1103/PhysRevD.88.085011.
- [43] Flachi, A.; Nitta, M.; Takada, S.; Yoshii, R. Sign Flip in the Casimir Force for Interacting Fermion Systems. *Phys. Rev. Lett.* **2017**, *119*, 031601. DOI:10.1103/PhysRevLett.119.031601.
- [44] Flachi, A.; Vitagliano, V. Symmetry breaking and lattice kirigami: Finite temperature effects. *Phys. Rev. D* **2019**, *99*, 125010. DOI:10.1103/PhysRevD.99.125010.
- [45] Bellucci, S.; Saharian, A.A. Fermionic Casimir densities in toroidally compactified spacetimes with applications to nanotubes. *Phys. Rev. D* **2009**, *79*, 085019. DOI:10.1103/PhysRevD.79.085019.
- [46] Bellucci, S.; Saharian, A.A.; Bardeghyan, V.M. Induced fermionic current in toroidally compactified spacetimes with applications to cylindrical and toroidal nanotubes. *Phys. Rev. D* **2010**, *82*, 065011. DOI:10.1103/PhysRevD.82.065011.
- [47] Bellucci, S.; Bezerra de Mello, E.R.; Saharian, A.A. Finite temperature fermionic condensate and currents in topologically nontrivial spaces. *Phys. Rev. D* **2014**, *89*, 085002. DOI:10.1103/PhysRevD.89.085002.
- [48] Bellucci, S.; Saharian, A.A. Fermionic Casimir effect for parallel plates in the presence of compact dimensions with applications to nanotubes. *Phys. Rev. D* **2009**, *80*, 105003. DOI:10.1103/PhysRevD.80.105003.
- [49] Elizalde, E.; Odintsov, S.D.; Saharian, A.A. Fermionic condensate and Casimir densities in the presence of compact dimensions with applications to nanotubes. *Phys. Rev. D* **2011**, *83*, 105023. DOI:10.1103/PhysRevD.83.105023.
- [50] Bellucci, S.; Saharian, A.A. Fermionic current from topology and boundaries with applications to higher-dimensional models and nanophysics. *Phys. Rev. D* **2013**, *87*, 025005. DOI:10.1103/PhysRevD.87.025005.
- [51] Bezerra de Mello, E.R.; Saharian, A.A. Casimir Effect in Hemisphere Capped Tubes. *Int. J. Theor. Phys.* **2016**, *55*, 1167. DOI:10.1007/s10773-015-2758-0.
- [52] Bellucci, S.; Saharian, A.A.; Vardanyan, V. Fermionic currents in AdS spacetime with compact dimensions. *Phys. Rev. D* **2017**, *96*, 065025. DOI:10.1103/PhysRevD.96.065025.

- [53] Bellucci, S.; Saharian, A.A.; Simonyan, D.H.; Vardanyan, V. Fermionic currents in topologically nontrivial braneworlds. *Phys. Rev. D* **2018**, *98*, 085020. DOI:10.1103/PhysRevD.98.085020.
- [54] Bellucci, S.; Saharian, A.A.; Sargsyan, H.G.; Vardanyan, V. Fermionic vacuum currents in topologically nontrivial braneworlds: Two-brane geometry. *Phys. Rev. D* **2020**, *101*, 045020. DOI:10.1103/PhysRevD.101.045020.
- [55] Kolesnikov, D.V.; Osipov, V.A. Field-theoretical approach to the description of electronic properties of carbon nanostructures. *Phys. Part. Nucl.* **2009**, *40*, 502. DOI:10.1134/S1063779609040030.
- [56] Vozmediano, M.A.H.; Katsnelson, M.I.; Guinea, F. Gauge fields in graphene. *Phys. Rep.* **2010**, *496*, 109. DOI:10.1016/j.physrep.2010.07.003.
- [57] Iorio, A.; Lambiase, G. Quantum field theory in curved graphene spacetimes, Lobachevsky geometry, Weyl symmetry, Hawking effect, and all that. *Phys. Rev. D* **2014**, *90*, 025006. DOI:10.1103/PhysRevD.90.025006.
- [58] Morresi, T.; et. al. Exploring event horizons and Hawking radiation through deformed graphene membranes. *2D Mater.* **2020**, *7*, 041006. DOI:10.1088/2053-1583/aba448.
- [59] Bellucci, S.; Brevik, I.; Saharian, A.A.; Sargsyan, H.G. The Casimir effect for fermionic currents in conical rings with applications to graphene ribbons. *Eur. Phys. J. C* **2020**, *80*, 281. DOI:10.1140/epjc/s10052-020-7819-8.
- [60] Krishnan, A.; et. al. Graphitic cones and the nucleation of curved carbon surfaces. *Nature* **1997**, *388*, 451. DOI:10.1038/41284.
- [61] Charlier, J.-Ch.; Rignanes, G.-M. Electronic Structure of Carbon Nanocones. *Phys. Rev. Lett.* **2001**, *86*, 5970. DOI:10.1103/PhysRevLett.86.5970.
- [62] Naess, S.N.; Elgsaeter, A.; Helgesen, G.; Knudsen, K.D. Carbon nanocones: wall structure and morphology. *Sci. Technol. Adv. Mater.* **2009**, *10*, 065002. DOI:10.1088/1468-6996/10/6/065002.
- [63] Lammert, P.E.; Crespi, V.H. Topological Phases in Graphitic Cones. *Phys. Rev. Lett.* **2000**, *85*, 5190. DOI:10.1103/PhysRevLett.85.5190.
- [64] Osipov, V.A.; Kochetov, E.A. Dirac fermions on graphite cones. *JETP Letters* **2001**, *73*, 562. DOI:10.1134/1.1387528.
- [65] Lammert, P.E.; Crespi, V.H. Graphene cones: Classification by fictitious flux and electronic properties. *Phys. Rev. B* **2004**, *69*, 035406. DOI:10.1103/PhysRevB.69.035406.
- [66] Cortijo, A.; Vozmediano, M.A.H. Effects of topological defects and local curvature on the electronic properties of planar graphene. *Nucl. Phys. B* **2007**, *763*, 293-308. DOI:10.1016/j.nuclphysb.2006.10.031.
- [67] Sitenko, Yu.A.; Vlasii, N.D. Electronic properties of graphene with a topological defect. *Nucl. Phys. B* **2007**, *787*, 241-259. DOI:10.1016/j.nuclphysb.2007.06.001.
- [68] Sitenko, Yu.A.; Vlasii, N.D. On the possible induced charge on a graphitic nanocone at finite temperature. *J. Phys. A: Math. Theor.* **2008**, *41*, 164034. DOI:10.1088/1751-8113/41/16/164034.
- [69] Furtado, C.; Moraes, F.; Carvalho, A.M.M. Geometric phases in graphitic cones. *Phys. Lett. A* **2008**, *372*, 5368-5371. DOI:10.1016/j.physleta.2008.06.029.

- [70] Chakraborty, B.; Gupta, K.S.; Sen, S. Effect of topology on the critical charge in graphene. *Phys. Rev. B* **2011**, *83*, 115412. DOI:10.1103/PhysRevB.83.115412.
- [71] Sitenko, Yu.A.; Vlasii, N.D. Vacuum polarization in graphene with a topological defect. *Low Temp. Phys.* **2008**, *34*, 826. DOI:10.1063/1.2981397.
- [72] Sitenko, Yu.A.; Gorkavenko, V.M. Properties of the ground state of electronic excitations in carbon-like nanocones. *Low Temp. Phys.* **2018**, *44*, 1261. DOI:10.1063/1.5078524.
- [73] Sitenko, Yu.A.; Gorkavenko, V.M. Induced vacuum magnetic flux in quantum spinor matter in the background of a topological defect in two-dimensional space. *Phys. Rev. D* **2019**, *100*, 085011. DOI:10.1103/PhysRevD.100.085011.
- [74] Bellucci, S.; Bezerra de Mello, E.R.; Saharian, A.A. Fermionic condensate in a conical space with a circular boundary and magnetic flux. *Phys. Rev. D* **2011**, *83*, 085017. DOI:10.1103/PhysRevD.83.085017.
- [75] Bezerra de Mello, E.R.; Bezerra, V.; Saharian, A.A.; Bardeghyan, V.M. Fermionic current densities induced by magnetic flux in a conical space with a circular boundary. *Phys. Rev. D* **2010**, *82*, 085033. DOI:10.1103/PhysRevD.82.085033.
- [76] Bezerra de Mello, E.R.; Moraes, F.; Saharian, A.A. Fermionic Casimir densities in a conical space with a circular boundary and magnetic flux. *Phys. Rev. D* **2012**, *85*, 045016. DOI:10.1103/PhysRevD.85.045016.
- [77] Bellucci, S.; Bezerra de Mello, E.R.; Bragança, E.; Saharian, A.A. Finite temperature fermion condensate, charge and current densities in a (2+1)-dimensional conical space. *Eur. Phys. J. C* **2016**, *76*, 350. DOI:10.1140/epjc/s10052-016-4195-5.
- [78] Saharian, A.A.; Bezerra de Mello, E.R.; Saharyan, A.A. Finite temperature fermionic condensate in a conical space with a circular boundary and magnetic flux. *Phys. Rev. D* **2019**, *100*, 105014. DOI:10.1103/PhysRevD.100.105014.
- [79] Chu, C.-S.; Miao, R.-X. Fermion condensation induced by the Weyl anomaly. *Phys. Rev. D* **2020**, *102*, 046011. DOI:10.1103/PhysRevD.102.046011.
- [80] Chu, C.-S.; Miao, R.-X. Weyl anomaly induced Fermi condensation and holography. *J. High Energy Phys.* **2020**, *2008*, 134. DOI:10.1007/JHEP08(2020)134.
- [81] Bellucci, S.; Saharian, A.A.; Grigoryan, A.Kh. Induced fermionic charge and current densities in two-dimensional rings. *Phys. Rev. D* **2016**, *94*, 105007. DOI:10.1103/PhysRevD.94.105007.
- [82] Johnson, K. The MIT bag model. *Acta Phys. Polonica* **1975**, *B6*, 865-892.
- [83] Berry, M.V.; Mondragon, R.J. Neutrino billiards: time-reversal symmetry-breaking without magnetic fields. *Proc. R. Soc. A* **1987**, *412*, 53-74. DOI:10.1098/rspa.1987.0080.
- [84] McCann, E., Fal'ko, V.I. Symmetry of boundary conditions of the Dirac equation for electrons in carbon nanotubes. *J. Phys.: Condens. Matter* **2004**, *16*, 2371-2379. DOI:10.1088/0953-8984/16/13/016.
- [85] Brey, L.; Fertig, H.A. Electronic states of graphene nanoribbons studied with the Dirac equation. *Phys. Rev. B* **2006**, *73*, 235411. DOI:10.1103/PhysRevB.73.235411.
- [86] Akhmerov, A.R.; Beenakker, C.W.J. Boundary conditions for Dirac fermions on a terminated honeycomb lattice. *Phys. Rev. B* **2008**, *77*, 085423. DOI:10.1103/PhysRevB.77.085423.

- [87] Beneventano, C.G.; Santangelo, E.M. Boundary Conditions in the Dirac Approach to Graphene Devices. *Int. J. Mod. Phys.: Conf. Series* **2012**, *14*, 240-249. DOI:10.1142/S2010194512007362.
- [88] Sitenko, Yu.A. Casimir effect with quantized charged spinor matter in background magnetic field. *Phys. Rev. D* **2015**, *91*, 085012. DOI:10.1103/PhysRevD.91.085012.
- [89] Araújo, A.L.; Maciel, R.P.; Dornelas, R.G.F.; Varjas, D.; Ferreira, G.J. Interplay between boundary conditions and Wilson's mass in Dirac-like Hamiltonians. *Phys. Rev. B* **2019**, *100*, 205111. DOI:10.1103/PhysRevB.100.205111.
- [90] Bezerra de Mello, E.R.; Saharian, A.A. Spinor Casimir effect for concentric spherical shells in the global monopole spacetime. *Class. Quantum Grav.* **2006**, *23*, 4673-4691. DOI:10.1088/0264-9381/23/14/008.
- [91] Saharian, A.A. *The Generalized Abel-Plana Formula with Applications to Bessel Functions and Casimir Effect*; Report No. ICTP/2007/082; Yerevan State University Publishing House: Yerevan, RA, 2008; arXiv:0708.1187.
- [92] Abramowitz, M.; Stegun, I.A. (Eds.) *Handbook of Mathematical Functions*; Dover: New York, NY, USA, 1972.
- [93] Miransky, V.A.; Shovkovy, I.A. Quantum field theory in a magnetic field: From quantum chromodynamics to graphene and Dirac semimetals. *Phys. Rept.* **2015**, *576*, 1-209. DOI:10.1016/j.physrep.2015.02.003.
- [94] Shifman, M.A.; Vainshtein, A.I.; Zakharov, V.I. QCD and resonance physics. Theoretical foundations. *Nucl. Phys. B* **1979**, *147*, 385-447. DOI:10.1016/0550-3213(79)90022-1.
- [95] Saharian, A.A.; Kotanjyan, A.S.; Sargsyan, H.G. Electromagnetic field correlators and the Casimir effect for planar boundaries in AdS spacetime with application in braneworlds. *Phys. Rev. D* **2020**, *102*, 105014. DOI:10.1103/PhysRevD.102.105014.
- [96] Klimenko, K.G. Phase structure of generalized Gross-Neveu models. *Z. Phys. C* **1988**, *37*, 457-463. DOI:10.1007/BF01578141.
- [97] Rosenstein, B.; Warr, B.J.; Park, S.H. Thermodynamics of  $(2 + 1)$ -dimensional four-fermion models. *Phys. Rev. D* **1989**, *39*, 3088-3092. DOI:10.1103/PhysRevD.39.3088; Four-fermion theory is renormalizable in  $2+1$  dimensions. *Phys. Rev. Lett.* **1989**, *62*, 1433-1436. DOI:10.1103/PhysRevLett.62.1433.
- [98] Semenoff, G.W.; Wijewardhana, L.C.R. Dynamical mass generation in 3D four-fermion Theory. *Phys. Rev. Lett.* **1989**, *63*, 2633-2636. DOI:10.1103/PhysRevLett.63.2633; Dynamical violation of parity and chiral symmetry in three-dimensional four-Fermi theory. *Phys. Rev. D* **1992**, *45*, 1342-1354, DOI:10.1103/PhysRevD.45.1342.
- [99] Ebert, D.; Klimenko, K.G.; Kolmakov, P.B.; Zhukovsky V.Ch. Phase transitions in hexagonal, graphene-like lattice sheets and nanotubes under the influence of external conditions. *Ann. Phys.* **2016**, *371*, 254-286. DOI:10.1016/j.aop.2016.05.001.
- [100] Ebert, D.; Blaschke, D. Thermodynamics of a generalized graphene-motivated  $(2 + 1)$ D Gross-Neveu model beyond the mean field within the Beth-Uhlenbeck approach. *Prog. Theor. Exp. Phys.* **2019**, 123I01. DOI:10.1093/ptep/ptz110.
- [101] Drut, J.E.; Son, D.T. Renormalization group flow of quartic perturbations in graphene: Strong coupling and large-N limits. *Phys. Rev. B* **2008**, *77*, 075115. DOI:10.1103/PhysRevB.77.075115.

- [102] Juričić, V.; Herbut, I.F.; Semenoff, G.W. Coulomb interaction at the metal-insulator critical point in graphene. *Phys. Rev. B* **2009**, *80*, 081405(R). DOI:10.1103/PhysRevB.80.081405.
- [103] Herbut, I.F.; Juričić, V.; Vafek, O. Relativistic Mott criticality in graphene. *Phys. Rev. B* **2009**, *80*, 075432. DOI: 10.1103/PhysRevB.80.075432.
- [104] Vitale, P. Temperature-induced phase transitions in four-fermion models in curved space-time. *Nucl. Phys. B* **1999**, *551*, 490-510. DOI:10.1016/S0550-3213(99)00212-6.
- [105] Ebert, D.; Klimenko, K.G.; Tyukov, A.V.; Zhukovsky, V.C. Finite size effects in the Gross-Neveu model with isospin chemical potential. *Phys. Rev. D* **2008**, *78*, 045008. DOI:10.1103/PhysRevD.78.045008.
- [106] Abreu, L.M.; Malbouisson, A.P.C.; Malbouisson, J.M.C.; Santana, A.E. Finite-size effects on the chiral phase diagram of four-fermion models in four dimensions. *Nucl. Phys. B* **2009**, *819*, 127-138. DOI:10.1016/j.nuclphysb.2009.04.012.
- [107] Ebert, D.; Klimenko, K.G. Cooper pairing and finite-size effects in a Nambu–Jona-Lasinio-type four-fermion model. *Phys. Rev. D* **2010**, *82*, 025018. DOI:10.1103/PhysRevD.82.025018.
- [108] Khanna, F.C.; Malbouisson, A.P.C.; Malbouisson, J.M.C.; Santana, A.E. Phase transition in the massive Gross-Neveu model in toroidal topologies. *Phys. Rev. D* **2012**, *85*, 085015. DOI:10.1103/PhysRevD.85.085015.
- [109] Zahed, I.; Brown, G.E. The Skyrme model. *Phys. Rep.* **1986**, *142*, 1-102. DOI:10.1016/0370-1573(86)90142-0.
- [110] Hosaka, A.; Hiroshi, T. Chiral bag model for the nucleon. *Phys. Rep.* **1996**, *277*, 65-188. DOI:10.1016/S0370-1573(96)00013-0.
- [111] Novak, M.A.; Rho, M.; Zahed, I. *Chiral Nuclear Dynamics*; World Scientific: Singapore, 1996.